Ab initio calculations of surface phonons of the hydrogen-terminated Si(110)-(1×1) surface

H. M. Tütüncü[1,2], Ertuğrul Karaca[1] and G. P. Srivastava[3]

[1] *Sakarya Üniversitesi, Fen-Edebiyat Fakültesi, Fizik Bölümü, 54187, Adapazarı, Turkey*

[2] *Sakarya Üniversitesi, Biyomedikal, Manyetik ve Yarıiletken Malzemeler Araştırma Me rkezi (BIMAYAM), 54187, Adapazarı, Turkey*

[3] *School of Physics, University of Exeter, Stocker Road, Exeter EX4 4QL, UK*

Abstract

A first-principles study, using a linear-response approach based on the pseudopotential method and the generalized gradient approximation, has been made to examine the phonon spectrum of the hydrogen-terminated Si(110)-(1×1) surface. The calculated results compare very well with the results determined from a recent high-resolution electron-energy-loss spectroscopy measurement. In particular, the energy locations and polarization characteristics of the H-Si bond bending and H-Si stretching surface phonon modes have been determined and discussed in detail. The zone-centre splitting of the two H-Si stretching surface phonon modes is found to 2.4 meV, which compares very well with the experimental value of 1.9 meV.

Key words: Density functional theory; hydrogen-terminated surface; surface relaxation ; surface phonon

[1] Corresponding Author: H. M. Tütüncü Tel: +90 264 295 60 72 Fax: +90 264 295 59 50 e-Mail: tutuncu@sakarya.edu.tr

1 Introduction

Silicon has been among the most widely studied of semiconductors because of its importance to device physics. For more than two decades, countless number of experimental and theoretical works have been carried out on the structural and electronic properties of Si semiconductor surfaces. **Because mainly of structural characterisation difficulties [1], the Si(110) surface has not been as well studied as the Si(111)(7×7) and Si(001)(2×1) surfaces.** However, recently the Si(110) surface has attracted a great deal of interest, due in part because of general attention to the physical properties of the low index silicon surfaces, and also due to the convenience of using this as a substrate surface for fabricating the multi-gate field effect transistor [2–4]. It is well known that adsorbed hydrogen has a considerable effect on the Si growth process and that hydrogenation of surfaces in solution as a final step of cleaning is a main technological step to form oxygen-free stable surfaces. Electrochemical process [5], wet chemical process [6–8] and hydrogen gas deposition process [9] have been used to prepare the hydrogen-terminated Si(110) surface. High quality monohydride Si(110) surfaces have been prepared by atomic hydrogen adsorption. However, depending upon the atomic hydrogen dose and the sample temperature during exposure, differently reconstructed surface structures, such as H:Si(110)-(1×1), H:Si(110)-(1×5), and H:Si(110)-(3×2), have been prepared [9]. The atomic geometry of H:Si(110)-(1×) has been determined by scanning tunneling microscopy [5,7,8].

The vibrational properties of semiconductors surfaces have been in general the subject of intense research over the past twenty years because they are closely linked to surface relaxation, phase transition and relaxation process of electronically or vibrationally excited states. On the experimental side, Watanabe [6] has used infrared (IR) spectroscopy with multireflection attenuated total reflection (ATR), as well as polarized IR transmission spectroscopy in order to determine stretching and bending vibrations concerned with H adsorbed on Si(110). Eremtchenko and co-workers [9] have reported an investigation of the vibrational properties of clean and monohydride-terminated Si(110) surface, determined by means of high resolution electron loss spectroscopy (HREELS). Their results [9] supply the first available data on surface phonons and on the dispersion of H-Si stretching and bending bands at the Si(110) surface. Recently, Matsushita and co-workers [10] have measured the surface phonon dispersion curves for the H:Si(110)-(1×1) surface along the two high symmetry directions $\overline{\Gamma}$-$\overline{X}$ and $\overline{\Gamma}$-$\overline{X'}$. They observed that the H-Si stretching and bending modes, which show highly anisotropic dispersion, propagate along the $\overline{\Gamma}$-$\overline{X}$ direction with a one-dimensional signature.

On the theoretical side, the surface phonon dispersion curves for the H:Si(110)-(1×1) surface have been calculated by the semi-empirical total-energy method [11]. In this theoretical work, the total energy can be presented as a sum of band structure energy and a repulsive energy term. The first one is taken into account using the empirical-tight-binding method (ETBM) while the second one can be identified by short-ranged pair potentials in terms of fractional bond-length changes. In that

work all parameters describing the total energy ansatz for the H:Si(110)-(1×1) surface are inferred from their previous treatment of the H:Si(111)-(1×1) surface [12]. In general, theoretical results of Gräschus et al are in good accordance with the experimental results [6]. However, the zone-centre splitting of H-Si bond stretching phonon modes is strongly underestimated in their ETBM, which does not include polarization effects or direct H-H interaction. While analysing their experimental measurements of surface phonon dispersion results for H:Si(110)-(1×1), Matsushita and co-workers [10] have argued that a first-principles theoretical method, such as one based on the density functional theory that accounts for H-H interaction, is needed to fully understand their results.

Following the suggestion from Matsushita *et al*, we have undertaken a first-principles study of the structural and vibrational properties of the hydrogen-terminated Si(110)-(1×1) surface using a plane-wave pesudopotential method within the density functional theory. We compare our theoretically obtained surface phonon dispersion curves with the HREELS data obtained by Matsushita *et al* [10]. From an examination of the eigenvectors of the dynamical problem, the origin of H-Si bond stretching and H-Si bond bending phonon modes on this surfaces are explained clearly.

2 Method

All calculations were performed by using the Quantum Espresso package [13]. We have utilized the density-functional theory in the generalized gradient approximation (GGA) [13] to determine the electronic ground state. Particularly, Kohn-Sham equations [14] are solved self-consistently for a given atomic configuration using the exchange-correlation potential in the parametrization of Perdew-Burke-Ernzerhof (PBE) [15]. Norm-conserving pseudopotentials [16] are used to treat the interaction of ionic cores and valence electrons. The Kohn-Sham orbitals are expanded in a plane-wave basis set with a kinetic-energy cutoff of 40 Ry.

The bulk Si is described in the diamond structure while the hydrogen terminated Si(110)-(1×1) surface is modeled by using a supercell approach [17]. A supercell is formed to include 30 Si atoms located in a slab of 15 atomic layers, and a vacuum region along the surface normal (the [110] direction) equivalent of seven atomic layers. Both sides of the Si slab are terminated with H atoms in order to form a symmetric H:Si(110)-(1×1) slab. The lattice constant of the periodic slab configuration is fixed to the calculated value of 5.47 $\mathring{A}$ determined for the bulk lattice constant of diamond Si. The optimized atomic structure within the H:Si(110)-(1×1) slab is obtained by minimizing the total energy by means of reducing the Hellmann-Feyman forces. The relaxation progress is started from a configuration in which the substrate atoms are placed in their ideal positions. Hydrogen atoms are located in the two dangling bond directions. Nine special $\boldsymbol{k}$ points are chosen, using the Monkhorst-Pack scheme [18], for sampling the irreducible segment of the Brillouin zone. All atoms in the slab are free to relax, except the the Si atoms in the middle of slab which are kept frozen to avoid the slab from a translation. The equilibrium positions are calculated with

numerical uncertainty of less than 0.01 $\AA$ when all forces are less than 0.1mRy/a.u.

The surface phonon dispersion curves of H:Si(110)-(1×1) have been determined by means of the density functional perturbation theory [13]. Within this approach, the second-order derivatives of the total energy, for generating the dynamical matrices, are determined from the static linear response of the electrons to the alteration of the external potential corresponding to periodic movements of the atoms. The response of electrons is taken into account iteratively, until self-consistency is reached between the alteration of the charge density and the screened perturbing potential. In order to determine the surface phonon dispersion curves of H:Si(110)-(1×1), we have calculated nine dynamical matrices within the irreducible segment of the surface Brillouin zone. Then, two-dimensional Fourier interpolation is made to calculate surface phonons for any chosen $\boldsymbol{q}$ points.

In order to check the effect of long-range dispersive forces for this hydrogen-adsorbed surface system, we also made calculations of the zone-centre phonon modes by including the Tkatchenko-Scheffler form [19] of the van der Waals correction to the exchange-correlation functional.

3 Results

3.1 Atomic geometry

In order to procure a clear description of the surface vibrations, it is mandatory to designate self-consistently the atomic equilibrium positions of the relaxed surface. Thus, first, we will present the relaxed atomic structure of H:Si(110)-(1×1) surface. Fig. 1 illustrates a top and side view of our relaxed atomic geometry from our calculations. We have found that the top substrate Si atoms are close to their bulk-derived positions, while the Si atoms in the second and all deeper substrate layers actually stay in the bulk positions. Consequently, the Si-Si tetrahedral bonding configuration stays almost unchanged. However, the top substrate layer Si-Si bond length results as 2.351 $\AA$, which is slightly smaller than the closet Si-Si distance in crystal (2.368 $\AA$). The value of the H-Si bond length is found to be 1.502 $\AA$, which is slightly larger than the H-Si distance in the silane molecule (1.48 $\AA$) and larger than the sum of the covalent radii of H and Si (1.47 A) [20]. A similar observation has been made in the theoretical work of Gräschus et al [11].

3.2 Surface phonons

3.2.1 The surface vibrational spectrum

Because of our construction of two identical surfaces on the two sides of the H:Si(110)-(1×1) slab, the surface phonon modes should appear in pairs. However, in our cal-

culations, the splitting of these pairs is smaller than 0.05 meV. This splitting is less then the experimental error margin of 0.5 meV. Thus, we will present only one set of the surface results. Our results for the surface phonon dispersion curves are displayed in Fig. 2 along the two highly symmetric directions $\overline{\Gamma}$-$\overline{X}$ and $\overline{\Gamma}$-$\overline{X'}$. The hatched regions show the projection of the bulk phonon modes. The localized surface phonon modes are shown by solid lines while the resonant surface phonon modes are displayed with dashed lines. In general, our phonon results are found to be in pleasing agreement with the recent HREELS data [10], which are shown by blue circles. In particular, the agreement between the experimental [10] and our GGA results for the two highest surface optical phonon branches is excellent.

3.2.2 Zone centre phonons

In general, the surface phonon modes of H:Si(110)-(1×1) at the centre of the surface Brillouion zone ($\overline{\Gamma}$), as well as along $\overline{\Gamma}$-$\overline{X'}$, can be categorised according to the point group symmetry of the surface unit cell [17]. Consequently, atomic vibrations along the zig-zag chain direction ([$\overline{1}$10]) are represented as $A^{''}$ modes while the vibrations perpendicular to the zig-zag chain direction are labeled as $A^{'}$. Such as a clear categorisation can not be made along the symmetry direction $\overline{\Gamma}$-$\overline{X}$ in the surface Brillouin zone.

We now present our surface phonons results for H:Si(110)-(1×1) at the centre of the surface Brillouion zone ($\overline{\Gamma}$). The phonon modes and their polarization characteristics are summarised in Tab. 1. The calculated results are compared with previous theoretical calculations [11] and experimental [6,10] measurements. In general, we find our results to be in gratifying accordance with the recent HREELS measurements [10]. In particular, the calculated Si-H bond stretching (BSM) and Si-H bond bending phonon modes are in very good agreement with the experimental values [6,10]. The egienvector representations (atomic displacement patterns) of the H-Si bond stretching (BSM) and H-Si bond bending phonon (BBM) modes are shown in Fig. 3.

In our calculations, the energies of symmetric (S_s) and anti-symmetric (S_a) bond stretching phonon modes are found to be 259.90 meV and 257.50 meV. Although both of these are of the $A^{'}$ representation, S_s and S_a are in-phase and out-of-phase stretching modes, respectively. These bond stretching phonon modes have been observed at 259.10 meV and 256.80 meV by Watanabe [6] using attenuated-total-reflection infrared spectroscopic measurements, and at 259.10 meV and at 257.20 meV in the recent HREELS measurement [10]. The calculated theoretical splitting of these stretching phonon modes of 2.4 meV also compares well with the experimental result of 1.9 meV from the HREELS measurements by Matsushita et al [10]. However, this splitting, with the numerical value of 0.08 meV, is considerably underestimated in the theoretical work of Gräschus et al [11]. Clearly, our GGA calculations predict the energies of bond stretching phonon modes in much better agreement with the HREELS measurements than the semi-empirical total-energy scheme did. In our view, accurate prediction of the symmetric-antisymmetric gap provides a test on the quality of the theoretical treatment of interatomic forces in the surface layers.

While the present method includes all relevant interatomic forces corresponding to the equilibrium geometry determined from the total energy minimization scheme, the same is not the case in the scheme adopted in the calculations using the semi-empirical total-energy scheme in [11]. The implicit use of bulk interaction models for surface calculations in [11] may be questionable. Bulk interaction models, because of the bulk symmetry they use, include a number of simplifications and cancellations, which are not represented in such a way at the surface because of breaking of bulk symmetry at the surface. The difference can also be contributed by the polarization effects or direct H-H interaction on this surface, which are not considered in the theoretical work of Gräschus et al [11].

Besides the H-Si bond stretching modes, the most significant features seen in the phonon dispersion curves of the H:Si(110)-(1×1) surface are the H-Si bond bending phonon modes. The zone-centre energies of these bending phonon modes are calculated to be 75.58, 75.76, 78.68 and 78.90 meV. Clearly, the frequencies of these modes lie above the projection of the bulk phonon modes. Also, as can be seen from Fig. 3, for these bending modes the motion of the H atoms is perpendicular to the H-Si bonds. The in-phase bond-bending mode at 75.58 meV and the out-of-phase bending mode at 78.90 meV have the A'' representation. The in-phase bond-bending mode at 78.68 and the out-of-phase bending mode at 75.76 meV have the A' representation. These bond bending modes have been the subject of some debate in publications dealing with experimental studies and the theoretical work by Gräschus et al [11]. These publications represent the in-phase modes as B_i and $\bar{B}_i$, and the out-of-phase modes as B_o and $\bar{B}_o$. Due to symmetry constraints in their use of polarized infrared beams, Watanabe could only observe the $\bar{B}_i$ at 612 cm^{-1} and B_i at 643 cm^{-1}. The B_i mode was actually split due to a nonideal surface structure (with frequencies 617 cm^{-1} and 649 cm^{-1}, with an average of 643 cm^{-1}). From an analysis of their HREELS spectra, Matsushita *et al.* [10] assigned the B_o mode at 77.4 meV (624 cm^{-1}) and the B_i mode at 80.6 meV (650 cm^{-1}). Allowing for uncertainty in measured values and some degree of nonideal surface structure, we can consider the two sets of experimental results to be in agreement with each other.

As presented in Tab. 2, the results of splittings between the stretching modes and the bending modes obtained in the previous theoretical calculations are at variance with the results obtained from the two experimental techniques mentioned above. In particular, in the theoretical work by Gräschus et al [11] the splittings $\omega(S_s) - \omega(S_a)$ and $\omega(B_i) - \omega(B_o)$ are underestimated, and the splitting $\omega(B_i) - \omega(\bar{B}_i)$ is overestimated. The theoretical results obtained by the more accurate theoretical method employed in this work suggest that these splittings are much closer to the experimentally estimated values.

Tables 1 and 2 also show the zone-centre surface modes computed with the vdW-corrected exchange-correlation functional. It is found that the results for the stretch and bending modes do not individually change appreciably. This indicates that the H atoms are bonded with the surface Si atoms with strong covalent bonds. However, the difference between the frequencies of the out-of-plane bending modes B_0 and $\bar{B}_0$ (*viz.* $\omega(\bar{B}_0) -$

$\omega(B_0)$) changes by as much as 24%. This is due to decrease in $\omega(\bar{B}_0)$ and increase in $\omega(B_0)$.

3.2.3 Phonon modes away from the zone centre

In general, the calculated surface phonon branches along the $\overline{\Gamma}$-$\overline{X'}$ symmetry directions agree well with the HREELS measurements by Matsushita *et al.* [10]. In particular, along the $\overline{\Gamma}$-$\overline{X'}$ symmetry direction, we have observed three acoustic surface localized phonon branches. The zone boundary energies of these acoustic branches are found to be 11.65, 11.85 and 14.01 meV. The egienvector representations of these acoustic branches are displayed in Fig. 4. The intermediate acoustic phonon mode at 11.85 meV has the A'' representation, while the other two branches are linked to atomic vibrations perpendicular to the zig-zag chain direction. The lowest acoustic phonon mode is known as the Rayleigh wave (RW) branch in the literature. The atomic vibrational pattern of RW mode at the $\overline{X'}$ point can be pictured as the motion of surface-layer H atoms with components in both the [110] and [001] directions, and of the first substrate layer Si atoms along the [001] direction. It is worth mentioning that as the three acoustic surface localized phonon branches mix strongly with bulk phonons close to the zone-centre Γ point, it is very difficult to identify these long wavelength modes. A similar observation has been made in the theoretical work of Gräschus et al [11].

Along $\overline{\Gamma}$-$\overline{X'}$*:* We have found a stomach gap phonon mode at the $\overline{X'}$ point with an energy of 23.28 meV. As can be seen in Fig. 5, the atomic vibrational pattern of this localized stomach gap phonon mode is largely of the H-Si bond stretching character. In the energy range from 74 to 82 meV, there are four surface localized phonon modes with energies of 74.88, 75.87, 77.82 and 81.67 meV. We have displayed the atomic vibrational patterns of these phonon mods in Fig. 6. The lowest and highest ones have A' character while the surface phonon modes with a group symmetry representation A'' are found at energies of 75.87 and 77.82 meV. All these phonon modes include the H-Si bond bending character because the H atoms move perpendicular to the H-Si bonds. At the $\overline{X'}$ point, the energies of H-Si bond stretching modes are found to be 258.64 and 258.94 meV.

Along $\overline{\Gamma}$-$\overline{X}$*:* Along the symmetry direction $\overline{\Gamma}$-$\overline{X}$, it is favorable to characterise phonon modes as showing either sagittal plane (SP) or shear horizontal (SH) polarization. The saggital plane is designated as that plane including both the two-dimensional phonon wave vector and the surface normal vector, while shear horizontal vibrations are those which happen perpendicular to the saggital plane. As can be seen from Fig. 2, the RW only becomes a true localized state along $\overline{\Gamma}$-$\overline{X}$ close to the zone boundary point $\overline{X}$. The atomic vibrational pattern of the RW mode at this point is illustrated in Fig. 7. This phonon at 15.75 meV is 82% SP polarized and corresponds to the motion of one of H atoms with components in both the [110] and [001] directions, while other H atom vibrates along the zig-zag chain direction. Above the projection of the bulk phonon modes, we have observed three surface phonon modes at the zone boundary point $\overline{X}$. The energies of these phonon modes are calculated to be 75.39, 80.32 and 258.23 meV. The eigenvector representations of these surface

phonon modes are presented in Fig. 8. The lower bond-bending phonon mode at 75.39 is a true localized surface phonon mode with 51% SP polarization while the second one at 80.32 meV has 80% SP character. Finally, the highest surface optical phonon mode at 258.23 meV shows a bond-stretching character This phonon mode is characterized by the motion of one of the H atoms with components in both the [110] and [001] directions.

4 Summary and Conclusion

In a totally self-consistent way, we have expanded *ab initio* pseudopotential calculations to a system of periodically repeated slab scheme in order to determine the atomic geometry and the phonon dispersion curves of the H:Si(110)-(1×1) surface. The presently determined atomic geometry is used to calculate surface phonon modes on this surface by means of an *ab initio* linear response formalism. In contrast to the previous theoretical work by based on an empirical tight-binding scheme by Gräschus et al [11], which ignores polarization effects and direct H-H interactions, the present formalism accounts for all relevant interactions, except for van der Waals force leading to direct H-H interaction. The calculated phonon dispersion curves compare very well with the recent high-resolution electron-energy-loss spectroscopy results. Because of the large mass mismatch between silicon and hydrogen atoms, H-Si bond bending and H-Si bond stretching phonon branches are found to lie well above the projection of the bulk phonon modes. These branches accord very well with their experimental ones along the two highly symmetric directions $\overline{\Gamma}$-$\overline{X}$ and $\overline{\Gamma}$-$\overline{X'}$. Our results confirm the anisotropic nature of the dispersion of the stretch modes, as analysed by Matsushita *et al.* [10] from their HREELS data. Our results also reproduce the degeneracy of the stretch modes at the zone-edge point $\overline{\Gamma}$-$\overline{X}$.

The polarization characteristics of H-Si bond bending and H-Si bond stretching phonon modes have been presented and discussed in detail. In particular, we have found zone-centre splitting of two H-Si stretching surface phonon modes to be 2.4 meV which in good accordance with its experimental value of 1.9 meV. On the other hand, this splitting is strongly underestimated with the value 0.08 meV by the semi-empirical total-energy scheme calculations. As a consequence, we can state that our *ab initio* pseudopotential calculations estimate the dispersion and energies of bond stretching phonon branches much better than the semi-empirical total-energy scheme did. We believe that this difference is largely due to a proper treatment in the present *ab initio* study of interatomic force constants and effectively charges.

The effect of a dispersion-corrected exchange-correlation functional was examined by computing the zone-centre phonons. It was found that the results for the stretch and bending modes do not individually change appreciably. However, the difference between the frequencies of the out-of-plane bending modes B_0 and $\bar{B}_0$ (*viz.* $\omega(\bar{B}_0)-\omega(B_0)$) was found to change by as much as 24%.

5 Acknowledgement

Some of the calculations for this project were carried out using the computing facilities on the Intel Nehalem (i7) cluster (ceres) in the School of Physics, University of Exeter, United Kingdom.

References

[1] F. Jona, IBM J. Res. Dev. 9 (1965) 375.

[2] M. Yang, E. P. Gusev, M. Leong, O. Gluschenkov, D. C. Boyd, K. K. Chan, P. M. Kozolowski, C. P. D′Emic, R. M. Sicina, P. C. Jamison, and A. I. Chou, IEEE Electron Device Lett. 24 (2003) 339.

[3] A. Teramoto, T. Hamada, M. Yamamoto, P. Gaubert, H. Akahori, K. Nii, M. Hirayama, K. Arima, K. Endo, S. Sugawa, and T. Ohmi, IEEE Trans. Electron Devices 54 (2007) 1438.

[4] N. Seifert, B. Gill, S. Jahinuzzaman, J. Basile, V. Ambrose, Q. Shi, R. Allmon, and A. Bramnik, IEEE Trans. Nucl. Sci. 59 (2012) 2666.

[5] J. H. Ye, K. Kaji, and K. Itaya, J. Electrochem. Soc. 143 (1996) 4012.

[6] S. Watanabe, Surf. Sci. 351 (1996) 149.

[7] K. Arima, J. Katoh, and K. Endo, Appl. Phys. Lett. 85 (2004) 6254.

[8] K. Arima, J. Katoh, S. Horie, K. Endo, T. Ono, S. Sugawa, H. Akahori, A. Teramato, and T. Ohmi, J. Appl. Phys. 98 (2005) 103525.

[9] M. Eremtchenko, F. S. Tautz, R. Öttking, V. M. Polyakov, F. Schwierz, and G. Cherkashinin, Surf. Sci. 582 (2005) 159.

[10] S. Y. Matsushita, K. Matsui, H. Kato, T. Yamada and S. Suto, J. Chem. Phys. 140 (2014) 104709.

[11] V. Gräschus, A. Mazur, and J. Pollmann, Phys. Rev. B 56 (1997) 6482.

[12] B. Sandfort, A. Mazur, and J. Pollmann, Phys. Rev. B 51 (1995) 7139.

[13] P. Giannozzi, S. Baroni, N. Bonini, M. Calandra, R. Car, C. Cavazzoni, D. Ceresoli, G. L. Chiarotti, M. Cococcioni, I. Dabo, A.D. Corso, S. de Gironcoli, S. Fabris, G. Fratesi, R. Gebauer, U. Gerstmann, C. Gougoussis, A. Kokalj, M. Lazzeri, L. Martin-Samos, N. Marzari, F. Mauri, R. Mazzarello, S. Paolini, A. Pasquarello, L. Paulatto, C. Sbraccia, S. Scandolo, G. Sclauzero, A.P. Seitsonen, A. Smogunov, P. Umari and R.M. Wentzcovitch, J. Phys.: Condens. Matter 21 (2009) 395502.

[14] W. Kohn and L. J. Sham, Phys. Rev. 140 (1965) A1133.

[15] J. P. Perdew, K. Burke, and M. Ernzerhof, Phys. Rev. Lett. 77 (1996) 3865.

[16] R. Stumpf, X. Gonge and M. Scheffler, A List of Separable, Norm-conserving, Ab Initio Pseudopotentials (Fritz-Haber-Institut, Berlin, 1990).

[17] G. P. Srivastava, *Theoretical Modelling of Semiconductor Surfaces* (World Scientific, Singapore, 1999).

[18] H. J. Monkhorst and J. D. Pack , Phys. Rev. B 13 (1976) 5188.

[19] A. Tkatchenko and M. Scheffler, Phys. Rev. Lett. **102**, 073005 (2009).

[20] C. A. Coulson, *Valence* (Oxford University Press, London, 1961), p. 189.

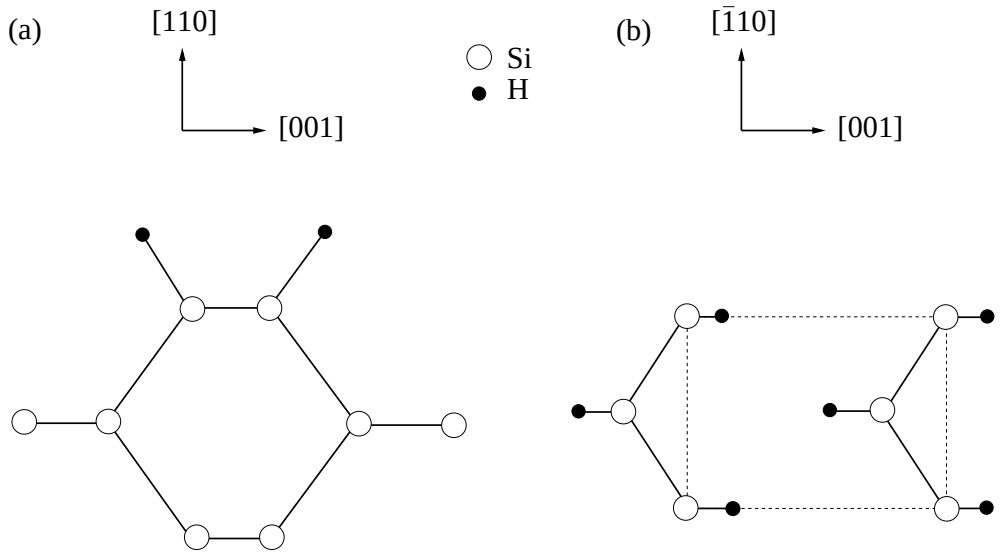

Fig. 1. Schematic (a) side and (b) top views of the relaxed surface geometry of the hydrogen-terminated Si(110)-(1×1) surface.

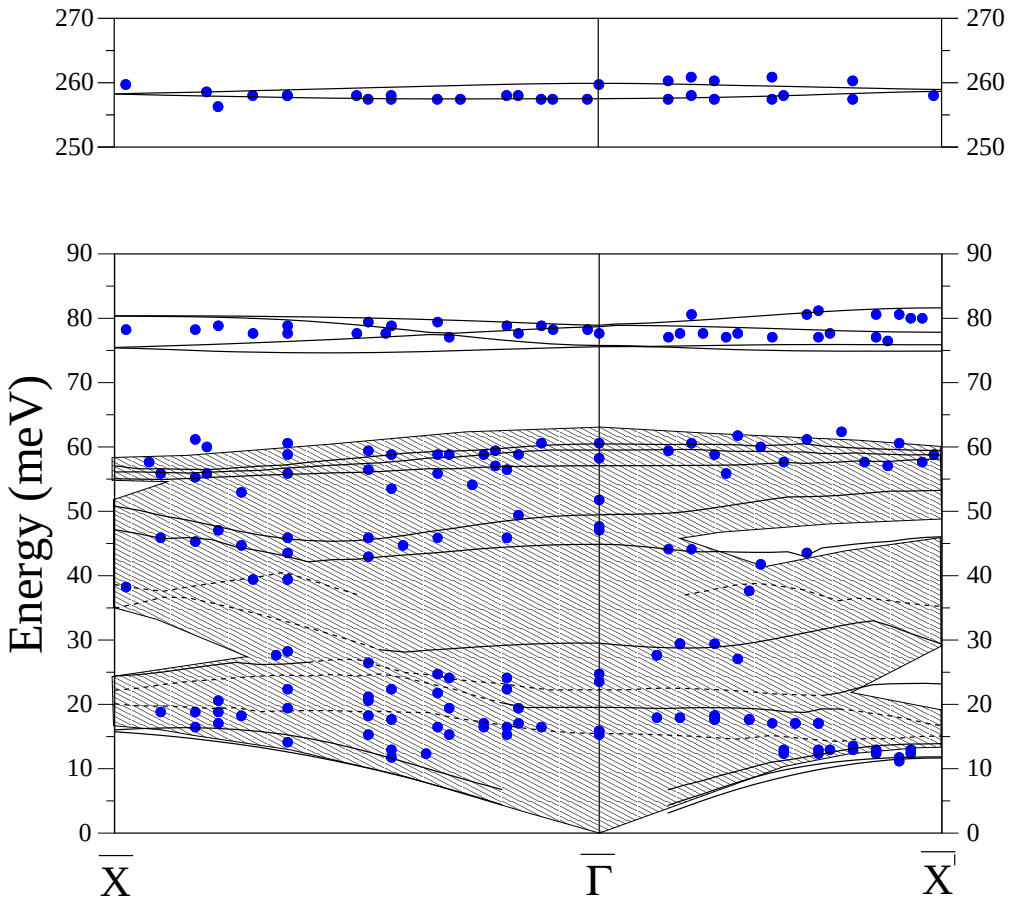

Fig. 2. The dispersion of phonon modes on the H:Si(110)-(1×1) surface. The black solid lines show the localized surface phonon branches while the black dashed line indicates the resonant surface phonon branches. The projected bulk phonon energies are shown as hatched regions while the blue circles show the experimental results from the high-resolution electron-energy loss sprectroscopy (HREELS) work of Matsushita *et al* [10].

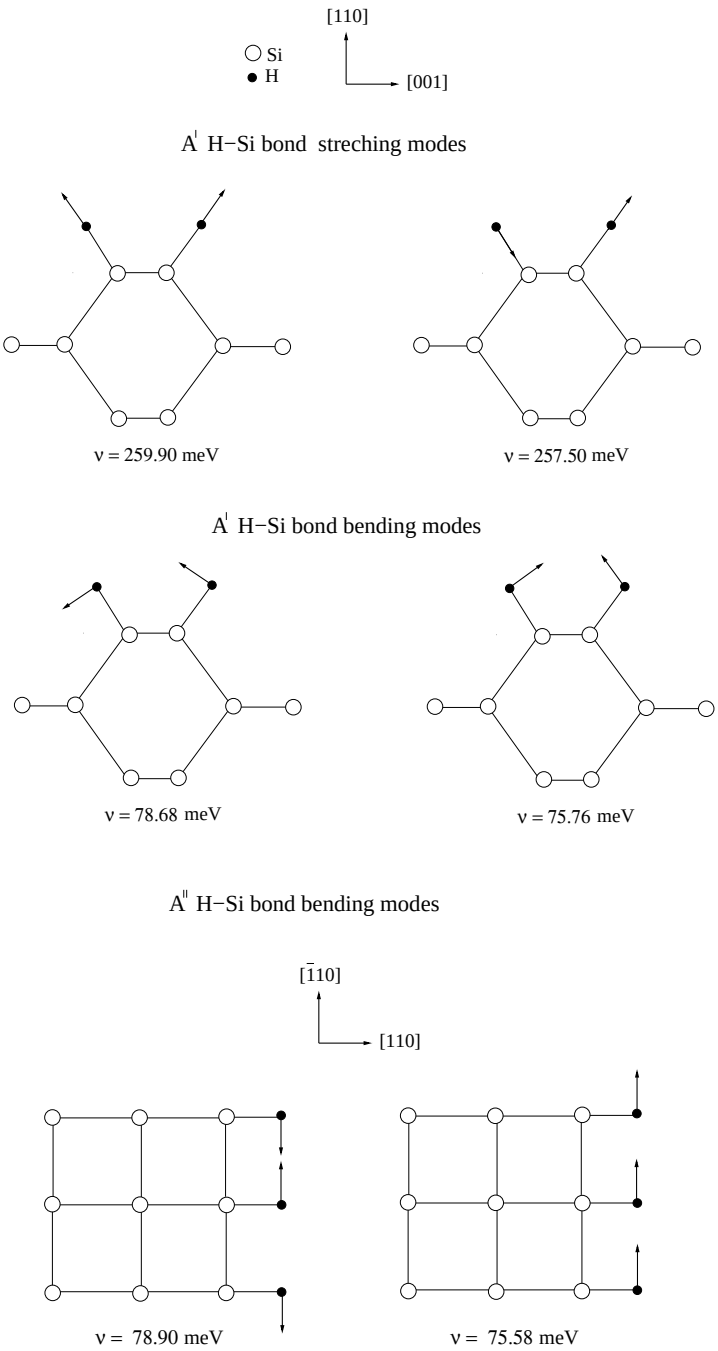

Fig. 3. Egienvector representations of H-Si bond stretching and H-Si bond bending phonon modes on the hydrogen-terminated Si(110)-(1×1) surface.

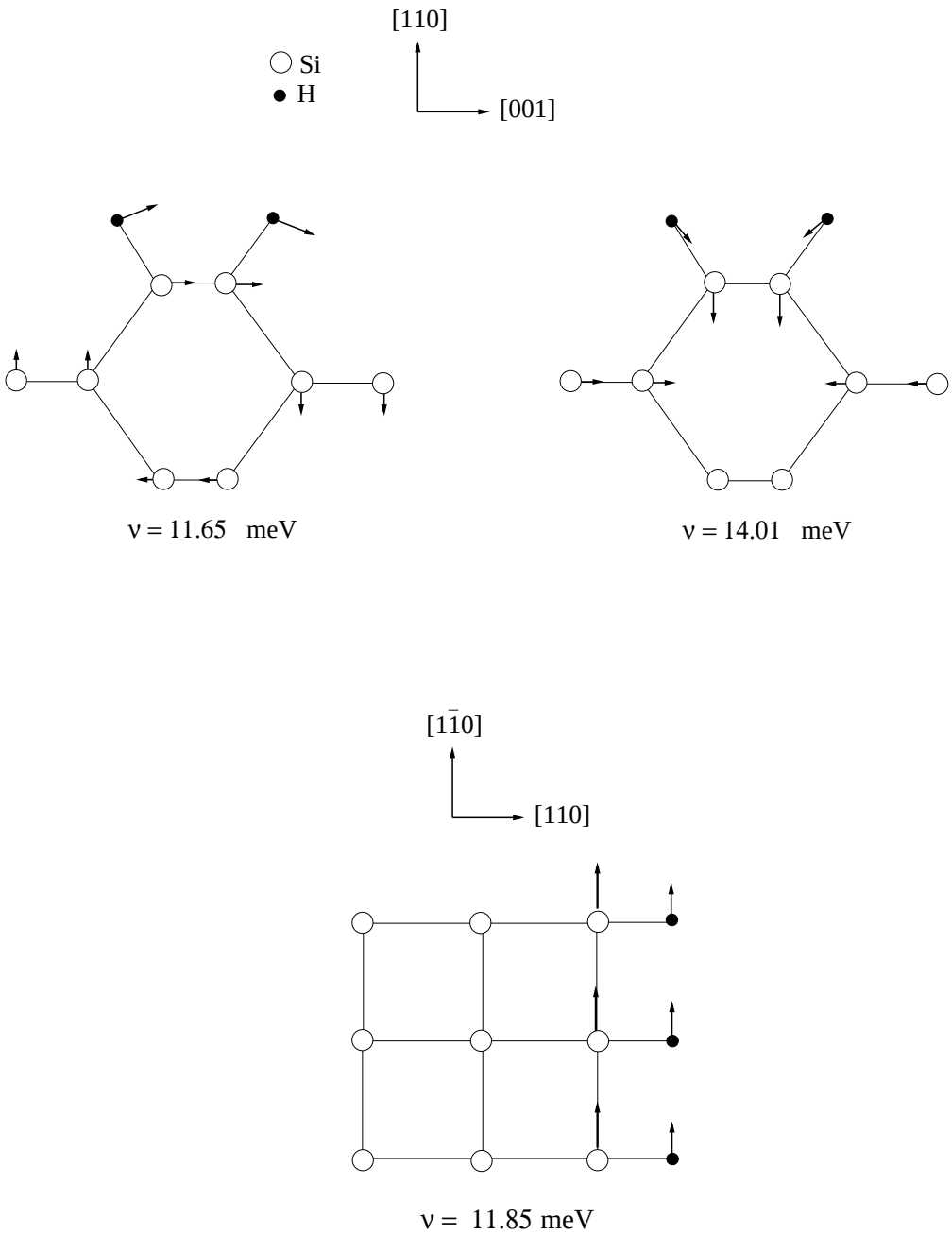

Fig. 4. Egienvector representations of three acoustic surface localized phonon modes for the hydrogen-terminated Si(110)-(1×1) surface at the $\overline{X'}$ point.

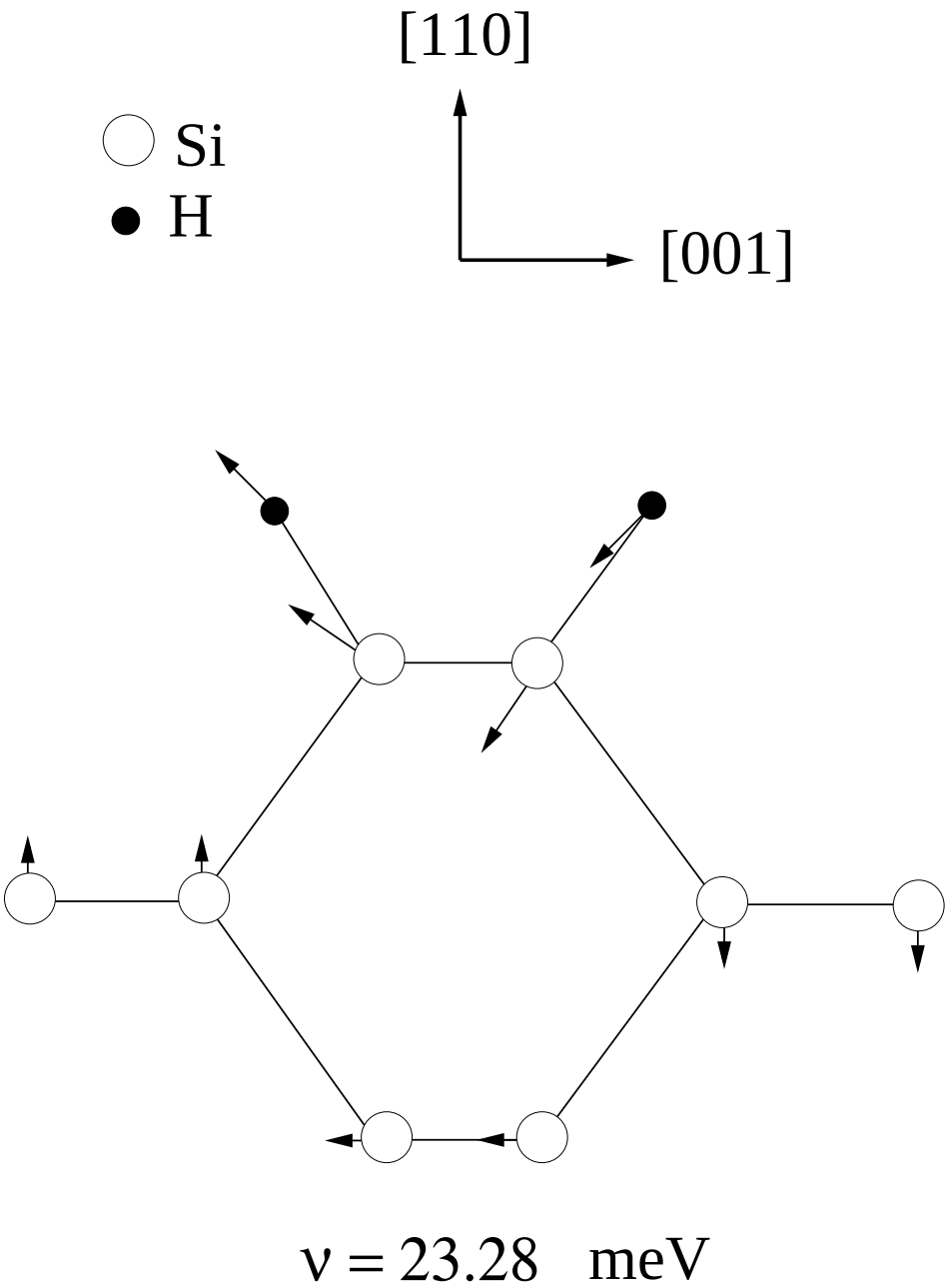

Fig. 5. Atomic vibrational pattern of the localized stomach gap phonon mode at the $\overline{X'}$ point for the H:Si(110)-(1×1) surface.

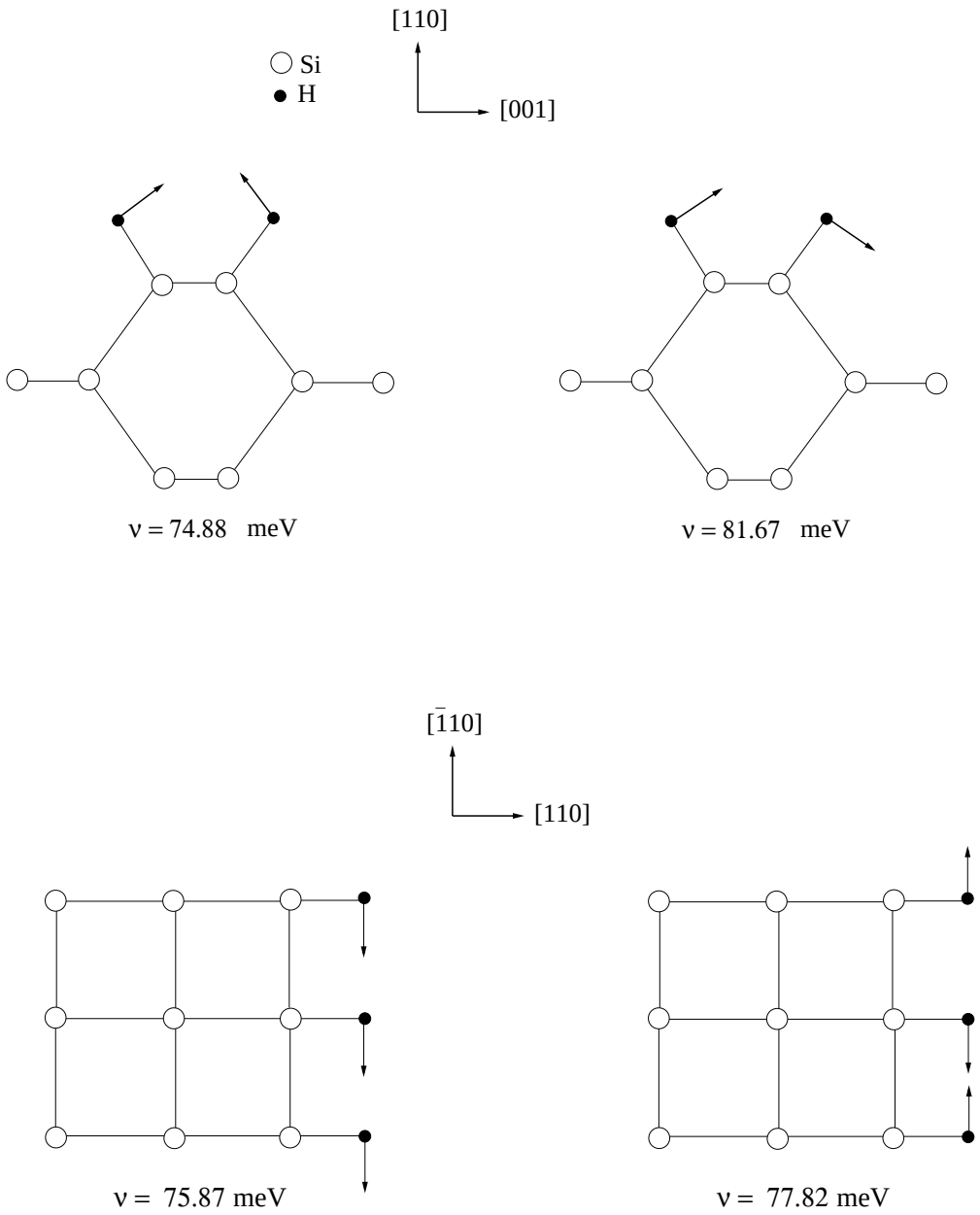

Fig. 6. Atomic vibrational patterns of H-Si bond bending phonon modes at the $\overline{X'}$ point for the H:Si(110)-(1×1) surface.

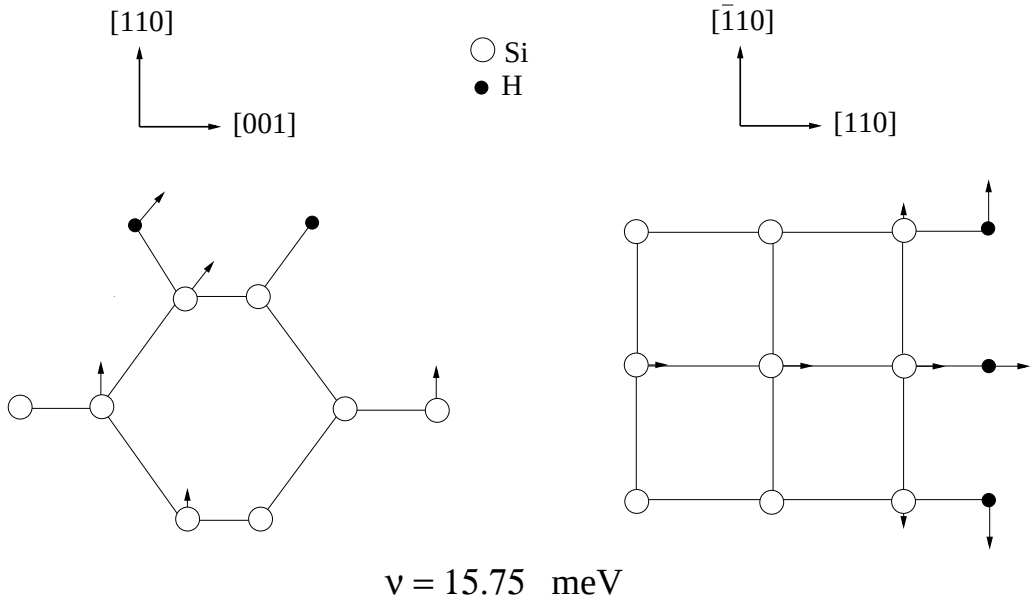

Fig. 7. Atomic vibrational pattern of the Rayleigh wave (RW) phonon mode at the zone-edge point $\overline{X}$ for the H:Si(110)-(1×1) surface.

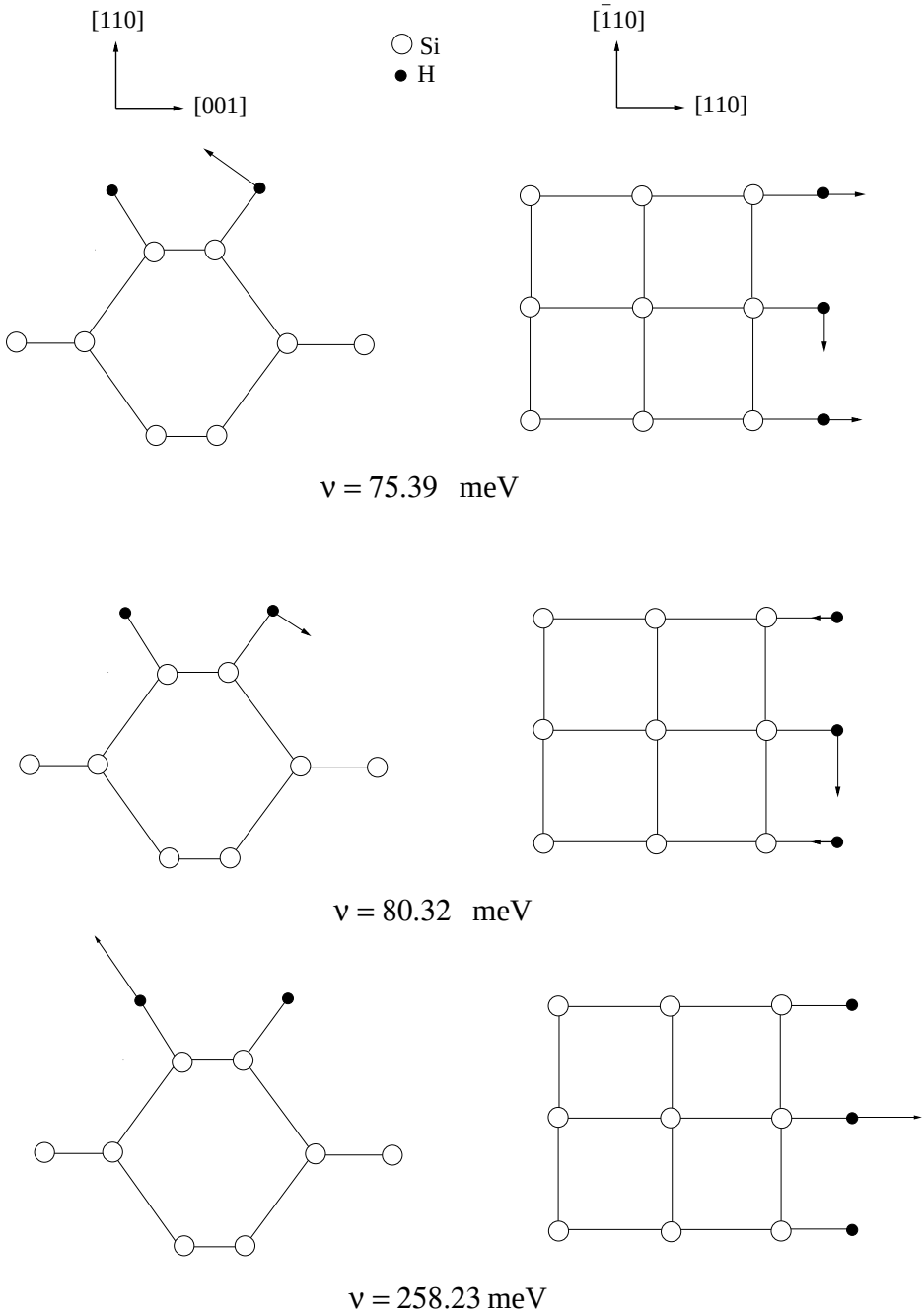

Fig. 8. Egienvector representations of H-Si bond bending modes and H-Si bond stretching phonon mode at the $\overline{X}$ point for the hydrogen-terminated Si(110)-(1×1) surface.

Table 1
Calculated surface phonon frequencies (in meV) on the H:Si(110)-(1×1) surface. The calculated surface phonon results are compared with previous theoretical and experimental results. BSM and BBM show H-Si bond stretching and H-Si bond bending modes, respectively. **vdW shows the results with the Tkatchenko-Scheffler form of the van der Waals interaction included.**

Source		A″					A′				
This work	57.08	75.58	78.90	29.56	44.87	49.45	60.40	75.76	78.68	257.50	259.90
This work with vdW	57.17	75.42	78.32	29.63	44.67	49.65	60.20	76.05	78.07	257.44	260.15
TB [11]	52.65	73.52	80.46	29.90	45.16	48.22	59.31	75.88	78.10	257.31	257.23
Experimental [6]		75.90							79.75	256.80	259.10
Experimental [10]	53.20			29.30	46.20	46.50	61.20	77.40	80.60	257.20	259.10
This work		BBM	BBM					BBM	BBM	BSM	BSM

Table 2
Comparison of theoretical and experimental results for the zone-centre bond stretching and bon-bending modes on the H:Si(110)-(1×1) surface. **The results in the parentheses are obtained by including the Tkatchenko-Scheffler form of the van der Waals interaction included.**

Mode	Present theory (cm^{-1})	Previous theory (cm^{-1}) [11]	Experiment (cm^{-1}) [6]	Experiment (cm^{-1}) [10]
S_a	2077 (2076)	2075.4	2071	2074
S_s	2096 (2098)	2074.8	2089	2090
$\bar{B}_0$	636 (632)	649		
B_i	635 (635)	630	643	650
B_0	611 (613)	612		624
$\bar{B}_i$	610 (608)	593	612	
$\omega(S_s) - \omega(S_a)$	19 (22)	-0.6	19	16
$\omega(\bar{B}_0) - \omega(B_0)$	25 (19)	37		
$\omega(B_i) - \omega(\bar{B}_i)$	25 (27)	37	31	
$\omega(B_i) - \omega(B_o)$	24 (22)	18		26